

# Surfactant Aggregates at a Flat, Isotropic Hydrophobic Surface

J. L. Wolgemuth,<sup>†</sup> R. K. Workman,<sup>‡</sup> and S. Manne<sup>\*,†</sup>

Department of Physics and Department of Materials Science, University of Arizona,  
Tucson, Arizona 85721

Received July 22, 1999. In Final Form: January 4, 2000

We report results of surfactant aggregate morphologies at an amorphous hydrophobic surface whose roughness is small compared to the size of a micelle. Direct imaging by atomic force microscopy shows that single-chain ionic, nonionic, and zwitterionic surfactants, which form spherical micelles in solution, form globular aggregates consistent with half-micelles at an amorphous hydrophobic surface. This result is consistent with the expected isotropy of chain–surface interactions.

## Introduction

The self-assembly of soluble surfactants in free solution has been experimentally investigated and theoretically modeled for several decades,<sup>1</sup> but the direct determination of surfactant aggregation at interfaces is comparatively new.<sup>2,3</sup> Atomic force microscopy (AFM), using soft repulsive interactions, has in the past few years imaged the aggregate structures of a variety of surfactants (ionic, nonionic, and zwitterionic) at a variety of solid surfaces (hydrophilic and hydrophobic) in contact with aqueous micellar solutions.<sup>2–18</sup> Most investigations have used atomically flat model surfaces, often the ordered cleavage planes of layered solids such as mica and graphite.

On crystalline hydrophobic surfaces, early results<sup>3</sup> showed that interfacial self-assembly was determined

almost entirely by the crystalline anisotropy of the substrate. AFM images revealed aggregates in the form of parallel stripes oriented perpendicular to an underlying symmetry axis and spaced apart by roughly twice the length of a surfactant molecule. These were interpreted as half-cylindrical micelles, where the bottom row of molecules is oriented horizontally along a symmetry axis. This basic morphology has since been observed for a variety of charged<sup>3,6,10</sup> and uncharged surfactants,<sup>8,11,14</sup> over a surprisingly wide range of surfactant geometries. Surfactants capable of cylindrical curvature (i.e., exhibiting a bulk hexagonal phase) have generally self-assembled into oriented half-cylinders on crystalline hydrophobic surfaces. This high degree of surface control has been attributed to the anisotropy of interaction between the horizontal alkane tail and the crystalline surface.<sup>2</sup> As long as the tail exceeds a certain minimum length (found to be ~10 carbon atoms<sup>14,17</sup>), the linear contact area between the tail and surface enhances the direction sensitivity of the interaction, leading to easy adsorption directions along the symmetry axes.

In contrast to the above, little work has been reported on aggregate phases at *isotropic* hydrophobic surfaces. These are important for several reasons. As model surfaces, they impose a simpler boundary condition on self-assembly, facilitating the future comparison of theory to experiment. Furthermore, comparing aggregation at amorphous vs crystalline surfaces serves to distinguish between the influence of simple hard-wall confinement and specific interactions with the surface lattice. Finally, amorphous hydrophobic surfaces may shed light on surfactant behavior at the air–solution interface, which is also amorphous and hydrophobic.

Ducker et al.<sup>14</sup> have recently reported AFM results of nonionic surfactant aggregation at an amorphous hydrophobic surface, namely, a silica surface to which diethyloctylchlorosilane (DEOS) had been covalently attached. They observed repulsive forces consistent with the expected range of steric/entropic interactions of the ethylene oxide headgroups. Imaging with these forces revealed a featureless adsorbate layer consistent with a uniform monolayer. Here we report the self-assembly of single-chain surfactants at amorphous silica surfaces hydrophobized by covalent attachment of trimethylchlorosilane (TMCS). This silanating agent permits the preparation of an amorphous hydrophobic surface while introducing only a small roughness (equivalent to a methyl group) to the

<sup>†</sup> Department of Physics.

<sup>‡</sup> Department of Materials Science.

(1) Reviews: (a) Evans, D. F.; Wennerström, H. *The Colloidal Domain*; Wiley-VCH: New York, 1994; Chapter 4. (b) Israelachvili, J. N. *Intermolecular and Surface Forces*, 2nd ed.; Academic Press: London, 1992; Chapters 16 and 17. (c) Laughlin, R. G. *The Aqueous Phase Behavior of Surfactants*; Academic Press: London, 1994.

(2) Manne, S.; Cleveland, J. P.; Gaub, H. E.; Stucky, G. D.; Hansma, P. K. *Langmuir* **1994**, *10*, 4409–4413.

(3) Manne, S.; Gaub, H. E. *Science* **1995**, *270*, 1480–1482.

(4) Review: Manne, S.; Warr, G. G. In *Supramolecular Structure in Confined Geometries*; Manne, S., Warr, G. G., Eds.; ACS Press: Washington, DC, 1999; Chapter 1.

(5) Jaschke, M.; Butt, H. J.; Gaub, H. E.; Manne, S. *Langmuir* **1997**, *13*, 1381–1384.

(6) Manne, S.; Schäffer, T. E.; Huo, Q.; Hansma, P. K.; Morse, D. E.; Stucky, G. D.; Aksay, I. A. *Langmuir* **1997**, *13*, 6382–6387.

(7) Manne, S. *Prog. Colloid Polym. Sci.* **1997**, *103*, 226–233.

(8) Patrick, H. N.; Warr, G. G.; Manne, S.; Aksay, I. A. *Langmuir* **1997**, *13*, 4349–4356.

(9) Patrick, H. N.; Warr, G. G.; Manne, S.; Aksay, I. A. *Langmuir* **1999**, *15*, 1685–1692.

(10) Wanless, E. J.; Ducker, W. A. *J. Phys. Chem.* **1996**, *100*, 3207–3214.

(11) Ducker, W. A.; Grant, L. M. *J. Phys. Chem.* **1996**, *100*, 11507–11511.

(12) Grant, L. M.; Ducker, W. A. *J. Phys. Chem. B* **1997**, *101*, 5337–5345.

(13) Lamont, R.; Ducker, W. *J. Colloid Interface Sci.* **1997**, *191*, 303–311.

(14) Grant, L. M.; Tiberg, F.; Ducker, W. A. *J. Phys. Chem. B* **1998**, *102*, 4288–4294.

(15) Lamont, R. E.; Ducker, W. A. *J. Am. Chem. Soc.* **1998**, *120*, 7602–7607.

(16) Ducker, W. A.; Wanless, E. J. *Langmuir* **1999**, *15*, 160–168.

(17) Holland, N. B.; Ruegsegger, M.; Marchant, R. E. *Langmuir* **1998**, *14*, 2790–2795.

(18) Burgess, I.; Jeffrey, C. A.; Cai, X.; Szymanski, G.; Galus, Z.; Lipkowski, J. *Langmuir* **1999**, *15*, 2607–2616.

original silica surface. This avoids grafted alkyl chains (such as the octyl chain of DEOS), which can potentially intercalate surfactant molecules and give rise to a more pliable interface.<sup>19</sup> Thus, our choice of TMCS was dictated mainly by the end goal of a flat, amorphous, and *rigid* hydrophobic interface.

Our results show that single-chain surfactants give rise to discrete globular aggregates, roughly consistent with hemispherical or hemiellipsoidal micelles, at the TMCS-coated silica surface. Because the same surfactants form spherical micelles in solution, the perturbation of spontaneous curvature is smaller for isotropic hydrophobic surfaces than for crystals.

### Experimental Section

The amorphous native oxide layer on silicon wafers was used as the foundation for preparing amorphous hydrophobic surfaces. Chips from a Si(100) wafer were washed in 2-propanol, blown dry with dry nitrogen (>99.995%), and placed in a plastic Petri dish. A few drops of TMCS (Fluka, >99%, volume ~50  $\mu$ L) were placed on a cover slip inside the Petri dish, a few centimeters from the Si chips. The Petri dish cover was left slightly open and the TMCS allowed to evaporate. When evaporation was complete (~30 min), the Si chips were rinsed in three consecutive baths of ethanol (in order to remove unreacted TMCS and physisorbed dimers) and blown dry with dry nitrogen. These samples were stored covered until use. They exhibited a static contact angle of  $80 \pm 3^\circ$ , measured using a side-mounted optical microscope equipped with a video display. Some surfaces were cleaned by an alternate published technique<sup>14</sup> of immersion in a solution of  $\text{NH}_4\text{OH}$  and  $\text{H}_2\text{O}_2$ , followed by exposure to an ultraviolet lamp; both sets of samples gave similar AFM results.

Commercial surfactants were used as received from Fluka (>98% purity); the dimeric surfactant (described below) was a kind gift of Stucky et al. Solutions were prepared using nanopure water directly decanted from a commercial system (Barnstead, resistivity 18.3  $\text{M}\Omega$  cm). Surfactant concentrations were typically a few times the critical micelle concentration (cmc). Five types of single-chain surfactants were used: the cationic dodecyltrimethylammonium bromide (DTAB; cmc 16 mM); the dimeric  $\text{C}_{16}\text{H}_{33}\text{N}^+(\text{CH}_3)_2(\text{CH}_2)_3\text{N}^+(\text{CH}_3)_3\cdot 2\text{Br}^-$  (termed  $\text{C}_{16-3-1}$ ; cmc ~3 mM); the anionic sodium dodecyl sulfate (SDS; cmc 8 mM); the zwitterionic 3-(*N,N*-dimethyldodecylammonio)propanesulfonate (DDAPS; cmc 2.2 mM); and the nonionic octakis(ethylene glycol) monododecyl ether ( $\text{C}_{12}\text{E}_8$ ; cmc 0.05 mM).<sup>20</sup> All of these surfactants form spherical micelles in free solution. The double-chain surfactant didodecyltrimethylammonium bromide (DDAB; cmc 0.15 mM), which forms bilayers and vesicles in solution, was used as a control.

We used a commercial AFM (Digital Instruments, Dimension 3100) operating in soft contact (or precontact) mode. In this mode, the repulsive (electric double layer or steric/entropic) force signature associated with the surfactant adsorbate is itself used as the contrast mechanism during AFM scans.<sup>2</sup> Force curves were obtained before and after each image to ensure that the imaging force originated from the surfactant layer and not from hard contact with the sample surface. Images were obtained using commercial V-shaped cantilevers (Digital Instruments, type DNP-S), specifically the long thin variety with a nominal spring constant ~0.06 N/m. Imaging scan rates were in the range 3–5 Hz, and all images were unprocessed except for slope removal along the fast scan axis. All data were recorded at room temperature ( $27 \pm 2^\circ\text{C}$ ).

(19) For example, a recent study has shown that pure alkane liquids penetrate into and intercalate with alkyldimethylsilane monolayers covalently grafted to silica. See: Fadeev, A. Y.; McCarthy, T. J. *Langmuir* **1999**, *15*, 3759–3766.

(20) cmc Data are from: (a) Rosen, M. J. *Surfactants and Interfacial Phenomena*; Wiley: New York, 1974; pp 95–99. (b) Weers, J. G.; Rathman, J. F.; Axe, F. U.; Crichlow, C. A.; Foland, D. R.; Scheuing, D. R.; Wierseman, R. J.; Zielske, A. G. *Langmuir* **1991**, *7*, 854–867.

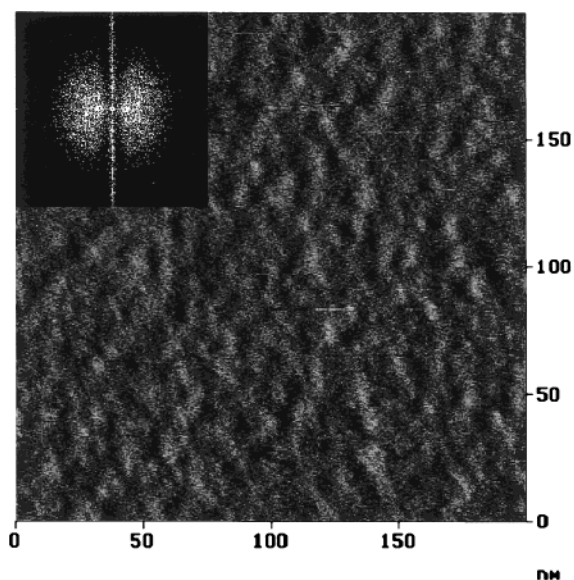


**Figure 1.**  $200 \times 200$  nm AFM image (contact mode) of TMCS-coated silica surface. The measured root-mean-square roughness of this entire area is 0.1 nm, and the average height of the undulations is 0.46 nm. These values are much smaller than typical micelle sizes (>4 nm). The FFT (inset) shows no pronounced periodicities.

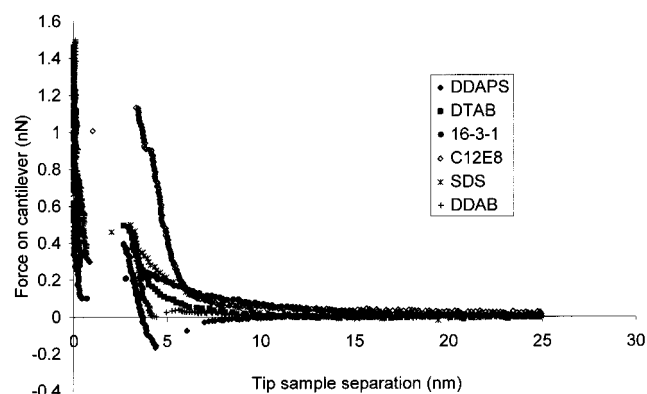


**Figure 2.** AFM approach curves on TMCS-coated silica for each surfactant used in this study (see text). The measured jump-in distances are listed in Table 1. Images in Figure 3 were obtained by maintaining a force setpoint in the repulsive precontact region of the force curve.

### Results and Discussion

The amorphous native oxide on silicon wafers typically shows disordered topographic undulations with elevations of a few angstroms and lateral peak spacings of order ~20 nm. These features are generally unavoidable; however, because their lateral extent is large (and their vertical extent small) in comparison to micelles, they have not seriously interfered with previous AFM investigations on bare silica surfaces.<sup>3,7,11,14</sup> The TMCS-coated surfaces (Figure 1) showed topography similar to bare silica, indicating that the surfaces were not significantly roughened by the covalent attachment.

Immersion in a surfactant solution gave rise to a long-range repulsion between tip and sample, similar to force curves previously reported for both charged and uncharged surfactants. Approach curves for the surfactants are shown in Figure 2. Repulsive interactions were roughly exponential and extended out to separations of around 10 nm. Forces reached values of order ~1 nN before rupture of the interfacial surfactant layers. Aggregate images were obtained by using a force setpoint below the rupture force;

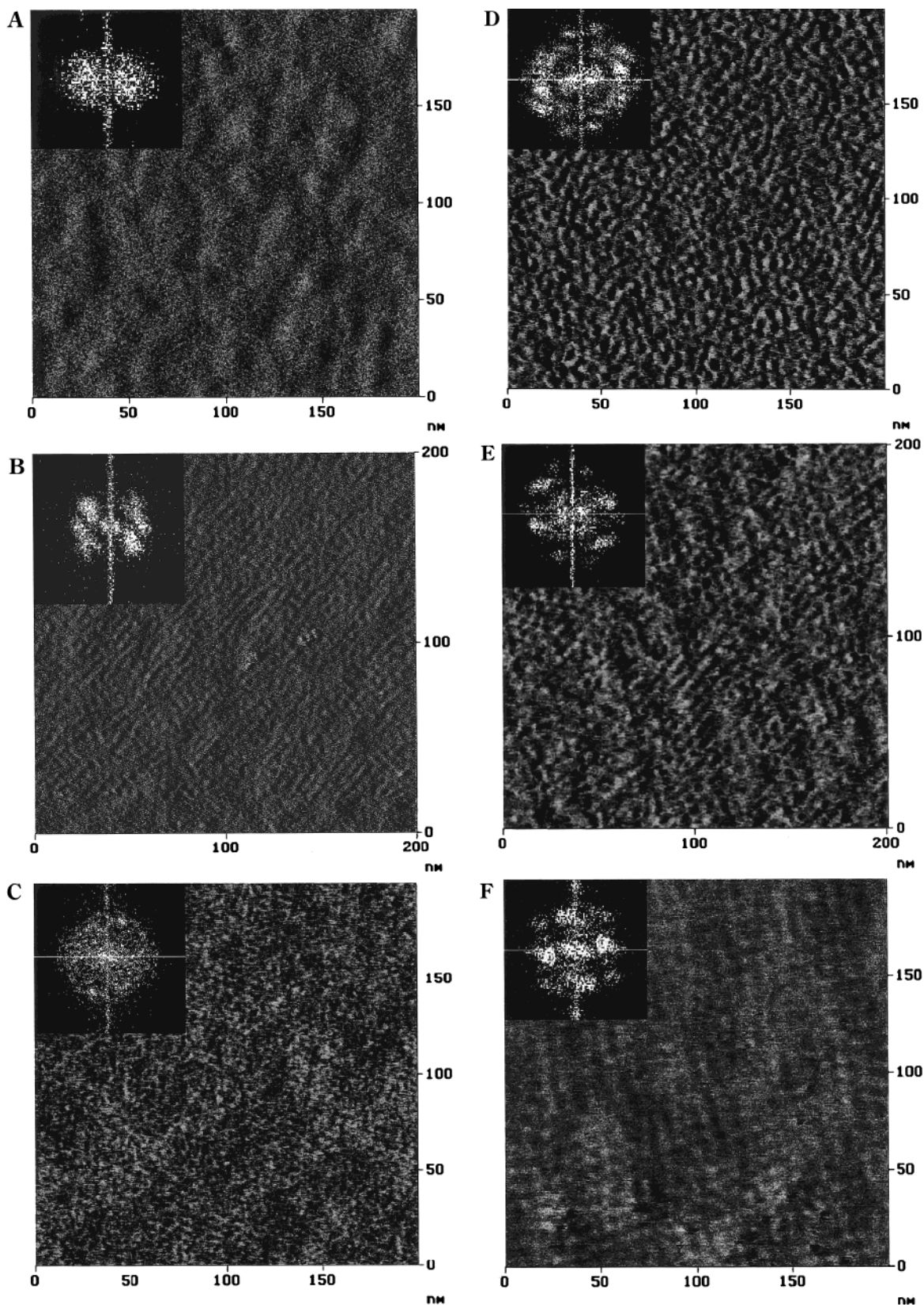


**Figure 3.**  $200 \times 200$  nm AFM images of adsorbed surfactants on TMCS-coated silica with fast Fourier transforms (FFTs, inset). (A) AFM scan of the double-chain surfactant DDAB (0.3 mM solution,  $2 \times \text{cmc}$ ) showing a surface that is virtually featureless, except for the underlying surface topography. (B) AFM scan of the cationic surfactant DTAB (32 mM solution,  $2 \times \text{cmc}$ ) showing globular and short linear aggregates over the underlying surface topography. The inset Fourier transform shows periodicities in the range  $4.4 \pm 0.3$  nm. (C) The zwitterionic surfactant DDAPS (10 mM solution,  $4.5 \times \text{cmc}$ ) also shows globular aggregates with an ill-defined periodicity in the range  $4.3 \pm 0.3$  nm. (D) The AFM scan of the dimeric surfactant  $C_{16-3-1}$  (3.0 mM solution) shows similarly globular structures with periodicities of  $6.7 \pm 0.4$  nm. (E) The nonionic surfactant  $C_{12}E_8$  (0.3 mM solution,  $6 \times \text{cmc}$ ) shows globular or short linear segments with periodicities of  $5.8 \pm 0.5$  nm. (F) The anionic surfactant SDS (50 mM solution,  $8 \times \text{cmc}$ ) shows globular aggregates at a comparatively large periodicity of  $9 \pm 2$  nm.

**Table 1. Surface Periodicities and Jump-in Distances for Surfactants on a Methylated Silica Surface**

surfactant	expected micelle diameter (nm) <sup>a</sup>	surface periodicity from FFTs (nm)	jump-in distance from force curves (nm)
DTAB	4.0	4.4 ± 0.3	2.7
DDAPS	4.3	4.3 ± 0.3	2.7
C <sub>12</sub> E <sub>8</sub>	5.1	5.8 ± 0.5	3.5
C <sub>16-3-1</sub>	6.0	6.7 ± 0.4	3.7
SDS	3.8	9 ± 2	3.0

<sup>a</sup> Micelle diameters were determined by doubling the length of the surfactant molecule (head + tail). The tail length was calculated from Tanford's formula (Tanford, C. *The Hydrophobic Effect*; Wiley: New York, 1973). For symmetric headgroups (SDS and DTAB), accepted values for ionic diameters were used; for short linear headgroups (DDAPS and C<sub>16-3-1</sub>), the average segment conformation was assumed to be approximately halfway between perpendicular to the tail and fully outstretched; for C<sub>12</sub>E<sub>8</sub> the headgroup size was assumed to be twice the Flory radius  $R_F \approx l n^{3/5}$ , where  $l$  is the monomer length for a (CH<sub>2</sub>-O-CH<sub>2</sub>) segment and  $n = 8$ . (For further discussion, see: reference 1b; pp 110 and 290.)

most images were rechecked at the lightest possible imaging forces to guard against tip-induced disruption of surfactant aggregates. Adsorbate features were also correlated between successive scans to ensure reproducibility.

Interfacial aggregate shape should be consistent with the range of spontaneous curvature accessible in solution. Therefore, double-chain surfactants such as DDAB serve as a useful control, because they can only form locally flat aggregates. AFM images of adsorbed DDAB on TMCS-coated silica (Figure 3A) show a layer which is featureless, except for the underlying sample topography, at all imaging forces. This is consistent with the expected flat monolayer, with tails pointing toward the substrate.

In contrast, single-chain ionic, nonionic, and zwitterionic surfactants appear to show globular aggregates on TMCS-silica (Figure 3B-F). These are visible as small closely spaced bumps superimposed on the larger-scale surface texture. Fast Fourier transforms (FFTs, inset) of these images allow us to quantify the aggregate morphology. Whereas the FFT of the DDAB image (Figure 3A) shows only a diffuse center spot (similar to the bare surface), FFTs of the single-chain surfactants express prominent periodicities that usually correspond well to the expected size range of micelles, as summarized in Table 1. Thus, the cationic DTAB and the zwitterionic DDAPS (parts B and C of Figure 3) both show FFT peaks at a little over 4 nm, agreeing well with the expected micelle diameters for these C<sub>12</sub> surfactants. The dimeric C<sub>16-3-1</sub>, with its longer 16-carbon chain and its doubly charged headgroup, gives rise to larger periodicities of 6.7 nm (Figure 3D), consistent with larger micelles. The nonionic C<sub>12</sub>E<sub>8</sub> (Figure 3E) also shows comparatively large spacings of 5.8 nm, as expected from its bulky ethylene oxide headgroup. The anionic SDS (Figure 3F) is the only exception, showing FFT periodicities of 9 ± 2 nm, which are anomalously large in comparison to its micelle diameter of ~4 nm. SDS spacings were also fairly variable between samples, with some samples adsorbing no SDS at all. These discrepancies are discussed below.

The images and FFTs also show that the aggregate phases are not well ordered. In some cases (Figure 3B-D) the FFTs show a nearly featureless ring, indicating an amorphous arrangement with a well-defined nearest-neighbor separation. In other cases (parts E and F of Figure 3), discrete but broad peaks are visible, suggesting some degree of local order in the way aggregates pack on the

amorphous surface. The observed order is far weaker than that for crystalline surfaces<sup>6</sup> and may be caused solely by interaggregate repulsive forces.

While AFM results have a high degree of lateral sensitivity, they must be compared to other techniques with high *vertical* sensitivity in order to arrive at a plausible aggregate morphology. Ellipsometry has shown that surfactants adsorb as a monolayer or submonolayer equivalent on hydrophobized silicon.<sup>21</sup> Neutron reflectometry has also revealed a submonolayer adsorbed thickness, indicating that chains must on average be tilted away from the surface normal.<sup>22</sup> When these are considered together with the AFM images, the most plausible aggregate structure that emerges is discrete half-micelles roughly in the form of hemispheres or hemiellipsoids. Such a morphology is perfectly consistent with the way in which the measured aggregate periodicity scales with expected micelle sizes (Table 1).

We also observe from Figure 2 that the jump-in distances for force curves (tabulated in the last column of Table 1) also increase with increasing micelle size. Although the absolute values of the jump-in distances should be interpreted with extreme caution, because the aggregate morphology on the tip surface is unknown before or after hemifusion, certainly the *trend* of increasing jump-in distances with increasing micelle size is also consistent with the proposed morphology of hemispherical micelles.

The scaling of aggregate periodicity with micelle size fails only in the case of SDS, where the measured lateral spacing is typically much greater than the micelle diameter and is not very reproducible between samples. We believe the reason lies with SDS having the same charge as ionizable SiOH groups left behind on the silica surface. There are two possible reasons for unreacted surface sites. First, they can result from suboptimal reaction conditions; the measured contact angles for the surfaces used herein are somewhat smaller than those reported in a recent systematic study of alkyl dimethylsilane monolayers.<sup>19</sup> Second, it has recently been pointed out<sup>23</sup> that, even when reaction conditions have been optimized, steric hindrance prevents monofunctional silanes such as TMCS from reacting with all of the hydroxyl groups on a silica surface, because the trimethylsilyl group is too bulky to match the surface density of SiOH groups. For these reasons, while reaction with TMCS makes the surface generally hydrophobic, some negative charge probably still exists, inhibiting SDS adsorption and giving rise to more open interaggregate spacings than for other surfactants. The putative role of surface charge is also consistent with control experiments on the cleavage plane of mica (not shown); on this highly negative surface, no SDS adsorption is observed even for solution concentrations up to ~100 times the cmc.

## Conclusion

Previous results showed that single-chain surfactants that aggregate into spherical micelles in solution self-assemble as half-cylinders at the crystalline hydrophobic interface, because of anisotropic interactions between the surface and tailgroup. The present results on amorphous

(21) Tibergh, F. *J. Chem. Soc., Faraday Trans.* **1996**, *92*, 531-538.  
 (22) Hines, J. D.; Fragneto, G.; Thomas, R. K.; Garrett, P. R.; Rennie, G. K.; Rennie, A. R. *J. Colloid Interface Sci.* **1997**, *189*, 259-267.  
 (23) Stevens, M. J. *Langmuir* **1999**, *15*, 2773-2778.

surfaces indicate that when this anisotropy is removed, spontaneous curvature reasserts itself, and interfacial aggregates become roughly hemispherical. Because similar morphologies occur over a wide range of headgroup types (both charged and uncharged), interfacial adsorption seems to be driven by hydrophobic interactions between the surface and tailgroups. When combined with the usual intermolecular interactions, this gives rise to an arrangement of globular half-micelles, with lateral periodicities that scale with expected micelle size. These results may serve as a useful guide for theoretical studies and

molecular dynamics simulations of surfactant behavior at unstructured hydrophobic walls.<sup>24,25</sup>

**Acknowledgment.** This work was supported by the University of Arizona Department of Physics and by a grant from Procter & Gamble Corp.

LA990986U

---

(24) Wijmans, C. M.; Linse, P. *J. Phys. Chem.* **1996**, *100*, 12583–12591.

(25) Bandyopadhyay, S.; Shelley, J. C.; Tarek, M.; Moore, P. B.; Klein, M. L. *J. Phys. Chem.* **1998**, *102*, 6318–6322.